



## Search for $CP$ violation in the decay $B^0 \rightarrow D^{*\pm} D^\mp$

T. Aushev,<sup>11</sup> Y. Iwasaki,<sup>7</sup> K. Abe,<sup>7</sup> K. Abe,<sup>39</sup> I. Adachi,<sup>7</sup> H. Aihara,<sup>41</sup> M. Akatsu,<sup>20</sup>  
Y. Asano,<sup>45</sup> T. Aziz,<sup>37</sup> S. Bahinipati,<sup>4</sup> A. M. Bakich,<sup>36</sup> A. Bay,<sup>16</sup> I. Bedny,<sup>1</sup> U. Bitenc,<sup>12</sup>  
I. Bizjak,<sup>12</sup> S. Blyth,<sup>24</sup> A. Bondar,<sup>1</sup> A. Bozek,<sup>25</sup> M. Bračko,<sup>18,12</sup> J. Brodzicka,<sup>25</sup> P. Chang,<sup>24</sup>  
Y. Chao,<sup>24</sup> A. Chen,<sup>22</sup> W. T. Chen,<sup>22</sup> B. G. Cheon,<sup>3</sup> R. Chistov,<sup>11</sup> Y. Choi,<sup>35</sup>  
A. Chuvikov,<sup>32</sup> M. Danilov,<sup>11</sup> M. Dash,<sup>46</sup> L. Y. Dong,<sup>9</sup> J. Dragic,<sup>19</sup> A. Drutskoy,<sup>4</sup>  
S. Eidelman,<sup>1</sup> V. Eiges,<sup>11</sup> Y. Enari,<sup>20</sup> F. Fang,<sup>6</sup> S. Fratina,<sup>12</sup> N. Gabyshev,<sup>1</sup> A. Garmash,<sup>32</sup>  
T. Gershon,<sup>7</sup> G. Gokhroo,<sup>37</sup> B. Golob,<sup>17,12</sup> N. C. Hastings,<sup>7</sup> K. Hayasaka,<sup>20</sup> M. Hazumi,<sup>7</sup>  
T. Higuchi,<sup>7</sup> L. Hinz,<sup>16</sup> T. Hokuue,<sup>20</sup> Y. Hoshi,<sup>39</sup> S. Hou,<sup>22</sup> W.-S. Hou,<sup>24</sup> T. Iijima,<sup>20</sup>  
A. Imoto,<sup>21</sup> K. Inami,<sup>20</sup> A. Ishikawa,<sup>7</sup> H. Ishino,<sup>42</sup> R. Itoh,<sup>7</sup> M. Iwasaki,<sup>41</sup> J. H. Kang,<sup>47</sup>  
J. S. Kang,<sup>14</sup> S. U. Kataoka,<sup>21</sup> N. Katayama,<sup>7</sup> H. Kawai,<sup>2</sup> T. Kawasaki,<sup>27</sup> H. R. Khan,<sup>42</sup>  
H. J. Kim,<sup>15</sup> S. K. Kim,<sup>34</sup> K. Kinoshita,<sup>4</sup> P. Koppenburg,<sup>7</sup> S. Korpar,<sup>18,12</sup> P. Krizán,<sup>17,12</sup>  
P. Krokovny,<sup>1</sup> C. C. Kuo,<sup>22</sup> A. Kuzmin,<sup>1</sup> Y.-J. Kwon,<sup>47</sup> J. S. Lange,<sup>5</sup> G. Leder,<sup>10</sup>  
S. H. Lee,<sup>34</sup> T. Lesiak,<sup>25</sup> J. Li,<sup>33</sup> S.-W. Lin,<sup>24</sup> D. Liventsev,<sup>11</sup> J. MacNaughton,<sup>10</sup>  
F. Mandl,<sup>10</sup> T. Matsumoto,<sup>43</sup> W. Mitaroff,<sup>10</sup> K. Miyabayashi,<sup>21</sup> H. Miyake,<sup>29</sup> H. Miyata,<sup>27</sup>  
R. Mizuk,<sup>11</sup> D. Mohapatra,<sup>46</sup> T. Mori,<sup>42</sup> T. Nagamine,<sup>40</sup> Y. Nagasaka,<sup>8</sup> E. Nakano,<sup>28</sup>  
M. Nakao,<sup>7</sup> H. Nakazawa,<sup>7</sup> Z. Natkaniec,<sup>25</sup> S. Nishida,<sup>7</sup> O. Nitoh,<sup>44</sup> S. Ogawa,<sup>38</sup>  
T. Ohshima,<sup>20</sup> T. Okabe,<sup>20</sup> S. Okuno,<sup>13</sup> S. L. Olsen,<sup>6</sup> W. Ostrowicz,<sup>25</sup> H. Ozaki,<sup>7</sup>  
P. Pakhlov,<sup>11</sup> H. Palka,<sup>25</sup> H. Park,<sup>15</sup> L. S. Peak,<sup>36</sup> L. E. Piilonen,<sup>46</sup> H. Sagawa,<sup>7</sup> Y. Sakai,<sup>7</sup>  
N. Sato,<sup>20</sup> T. Schietinger,<sup>16</sup> O. Schneider,<sup>16</sup> J. Schümann,<sup>24</sup> A. J. Schwartz,<sup>4</sup> S. Semenov,<sup>11</sup>  
K. Senyo,<sup>20</sup> M. E. Sevier,<sup>19</sup> H. Shibuya,<sup>38</sup> A. Somov,<sup>4</sup> N. Soni,<sup>30</sup> R. Stamen,<sup>7</sup>  
M. Starič,<sup>12</sup> K. Sumisawa,<sup>29</sup> T. Sumiyoshi,<sup>43</sup> O. Tajima,<sup>7</sup> F. Takasaki,<sup>7</sup> N. Tamura,<sup>27</sup>  
M. Tanaka,<sup>7</sup> G. N. Taylor,<sup>19</sup> Y. Teramoto,<sup>28</sup> K. Trabelsi,<sup>6</sup> T. Tsukamoto,<sup>7</sup> S. Uehara,<sup>7</sup>  
T. Uglov,<sup>11</sup> K. Ueno,<sup>24</sup> S. Uno,<sup>7</sup> G. Varner,<sup>6</sup> K. E. Varvell,<sup>36</sup> S. Villa,<sup>16</sup> C. C. Wang,<sup>24</sup>  
C. H. Wang,<sup>23</sup> B. D. Yabsley,<sup>46</sup> A. Yamaguchi,<sup>40</sup> Y. Yamashita,<sup>26</sup> J. Ying,<sup>31</sup> Y. Yuan,<sup>9</sup>  
S. L. Zang,<sup>9</sup> J. Zhang,<sup>7</sup> L. M. Zhang,<sup>33</sup> Z. P. Zhang,<sup>33</sup> V. Zhilich,<sup>1</sup> and D. Žontar<sup>17,12</sup>

(The Belle Collaboration)

- <sup>1</sup>*Budker Institute of Nuclear Physics, Novosibirsk*
- <sup>2</sup>*Chiba University, Chiba*
- <sup>3</sup>*Chonnam National University, Kwangju*
- <sup>4</sup>*University of Cincinnati, Cincinnati, Ohio 45221*
- <sup>5</sup>*University of Frankfurt, Frankfurt*
- <sup>6</sup>*University of Hawaii, Honolulu, Hawaii 96822*
- <sup>7</sup>*High Energy Accelerator Research Organization (KEK), Tsukuba*
- <sup>8</sup>*Hiroshima Institute of Technology, Hiroshima*
- <sup>9</sup>*Institute of High Energy Physics, Chinese Academy of Sciences, Beijing*
- <sup>10</sup>*Institute of High Energy Physics, Vienna*
- <sup>11</sup>*Institute for Theoretical and Experimental Physics, Moscow*
- <sup>12</sup>*J. Stefan Institute, Ljubljana*
- <sup>13</sup>*Kanagawa University, Yokohama*
- <sup>14</sup>*Korea University, Seoul*
- <sup>15</sup>*Kyungpook National University, Taegu*
- <sup>16</sup>*Swiss Federal Institute of Technology of Lausanne, EPFL, Lausanne*
- <sup>17</sup>*University of Ljubljana, Ljubljana*
- <sup>18</sup>*University of Maribor, Maribor*
- <sup>19</sup>*University of Melbourne, Victoria*
- <sup>20</sup>*Nagoya University, Nagoya*
- <sup>21</sup>*Nara Women's University, Nara*
- <sup>22</sup>*National Central University, Chung-li*
- <sup>23</sup>*National United University, Miao Li*
- <sup>24</sup>*Department of Physics, National Taiwan University, Taipei*
- <sup>25</sup>*H. Niewodniczanski Institute of Nuclear Physics, Krakow*
- <sup>26</sup>*Nihon Dental College, Niigata*
- <sup>27</sup>*Niigata University, Niigata*
- <sup>28</sup>*Osaka City University, Osaka*
- <sup>29</sup>*Osaka University, Osaka*
- <sup>30</sup>*Panjab University, Chandigarh*
- <sup>31</sup>*Peking University, Beijing*
- <sup>32</sup>*Princeton University, Princeton, New Jersey 08545*

<sup>33</sup>*University of Science and Technology of China, Hefei*

<sup>34</sup>*Seoul National University, Seoul*

<sup>35</sup>*Sungkyunkwan University, Suwon*

<sup>36</sup>*University of Sydney, Sydney NSW*

<sup>37</sup>*Tata Institute of Fundamental Research, Bombay*

<sup>38</sup>*Toho University, Funabashi*

<sup>39</sup>*Tohoku Gakuin University, Tagajo*

<sup>40</sup>*Tohoku University, Sendai*

<sup>41</sup>*Department of Physics, University of Tokyo, Tokyo*

<sup>42</sup>*Tokyo Institute of Technology, Tokyo*

<sup>43</sup>*Tokyo Metropolitan University, Tokyo*

<sup>44</sup>*Tokyo University of Agriculture and Technology, Tokyo*

<sup>45</sup>*University of Tsukuba, Tsukuba*

<sup>46</sup>*Virginia Polytechnic Institute and State University, Blacksburg, Virginia 24061*

<sup>47</sup>*Yonsei University, Seoul*

## Abstract

We report a search for  $CP$ -violating asymmetry in  $B^0 \rightarrow D^{*\pm} D^\mp$  decays. The analysis employs two methods of  $B^0$  reconstruction: full and partial. In the full reconstruction method all daughter particles of the  $B^0$  are required to be detected; the partial reconstruction technique requires a fully reconstructed  $D^-$  and only a slow pion from the  $D^{*+} \rightarrow D^0 \pi_{\text{slow}}^+$  decay. From a fit to the distribution of the time interval corresponding to the distance between two  $B$  meson decay points we calculate the  $CP$ -violating parameters and find the significance of nonzero  $CP$  asymmetry to be 2.7 standard deviations.

PACS numbers: 11.30.Er, 12.15.Hh, 13.25.Hw

In the Standard Model (SM),  $CP$  violation arises from the Kobayashi-Maskawa (KM) phase [1] in the weak interaction quark-mixing matrix. Comparisons between SM expectations and measurements in various modes are important to test the KM model. The  $B^0 \rightarrow D^{*\pm}D^\mp$  modes are of particular interest since large  $CP$  violation effects are expected in these decays [2]. Although the  $D^{*\pm}D^\mp$  final states are not  $CP$  eigenstates, they can be produced in the decays of both  $B^0$  and  $\bar{B}^0$  with comparable amplitudes; the interference between amplitudes of the direct transition and that via  $B\bar{B}$  mixing results in  $CP$  violation. These decays are dominated by the tree  $b \rightarrow c\bar{c}d$  transition, thus  $CP$  violation measurements are sensitive to the angle  $\phi_1$ . However, the  $b \rightarrow d$  penguin diagram also contributes to this final state and contains a different weak phase. Therefore this contribution results in both direct  $CP$  violation and a deviation of the mixing-induced  $CP$  violation parameter from  $\sin 2\phi_1$ . The Cabibbo suppressed decays  $B^0 \rightarrow D^{*\pm}D^\mp$  were first observed by Belle [3], and have been confirmed by *BABAR* [4].

The probability for a  $B$  meson to decay to  $D^{*\pm}D^\mp$  at time  $\Delta t$  can be expressed in terms of five parameters,  $\mathcal{A}$ ,  $S_\pm$  and  $C_\pm$ :

$$\mathcal{P}_{D^*D}^\pm(\Delta t) = (1 \pm \mathcal{A}) \frac{e^{-|\Delta t|/\tau_{B^0}}}{8\tau_{B^0}} \{1 + q[S_\pm \sin(\Delta m_d \Delta t) - C_\pm \cos(\Delta m_d \Delta t)]\}. \quad (1)$$

Here the  $+$ ( $-$ ) sign represents the  $D^{*+}D^-$  ( $D^{*-}D^+$ ) final state, and the  $b$ -flavor charge  $q = +1(-1)$  when the tagging  $B$  meson is a  $B^0(\bar{B}^0)$ . The time-integrated asymmetry  $\mathcal{A}$  between the rates to  $D^{*+}D^-$  and  $D^{*-}D^+$  is defined as

$$\mathcal{A} = \frac{N_{D^{*+}D^-} - N_{D^{*-}D^+}}{N_{D^{*+}D^-} + N_{D^{*-}D^+}}. \quad (2)$$

In the case of negligible penguin contributions [2, 5], the parameters  $S_\pm$  can be related to the weak phase difference ( $\sin 2\phi_1$  in the SM), the strong phase difference ( $\delta$ ) and the ratio of tree amplitudes to the  $D^{*+}D^-$  and  $D^{*-}D^+$  final states. If  $\delta = 0$  and equal amplitudes are assumed, one expects that  $\mathcal{A} = 0$ ,  $C_+ = C_- = 0$  and  $S_+ = S_- = -\sin 2\phi_1$ .

The analysis described here is based on  $140 \text{ fb}^{-1}$  of data, corresponding to  $152 \times 10^6$   $B\bar{B}$  pairs, collected with the Belle detector [6] at the KEKB asymmetric energy storage rings [7]. Two reconstruction techniques, full and partial, are used to increase the reconstruction efficiency. The event selection is similar to that in our previous publication [3], however some requirements are relaxed in order to increase the size of the sample used to extract the  $CP$  violation parameters. The full reconstruction method allows extraction of the signal

decay with high purity, but, due to the small branching fractions of charmed meson decays into reconstructable final states, results in a low efficiency. In the partial reconstruction method, a  $D^-$  meson is fully reconstructed while only the slow pion ( $\pi_{\text{slow}}^+$ ) is required to be detected from the decay  $D^{*+} \rightarrow D^0 \pi_{\text{slow}}^+$ .

Neutral  $D$  mesons are reconstructed in five decay modes:  $K^-\pi^+$ ,  $K^-\pi^+\pi^+\pi^-$ ,  $K^-\pi^+\pi^0$ ,  $K_S\pi^+\pi^-$  and  $K^+K^-$  [8]. Charged  $D$  mesons are reconstructed via decays into  $K^+\pi^-\pi^-$ ,  $K_S\pi^-$  and  $K^+K^-\pi^-$ . The selected combinations are fitted to a common vertex and a vertex quality requirement is applied to reduce combinatorial background. A  $\pm 15 \text{ MeV}/c^2$  interval around the nominal  $D$  mass is used to select  $D$  meson candidates for all modes except  $D^0 \rightarrow K^-\pi^+\pi^0$ , for which  $\pm 24 \text{ MeV}/c^2$  is used ( $\sim 3\sigma$  in each case). The selected charmed meson candidates are then subjected to mass-vertex constrained fits to improve their momentum and vertex resolution. We refer to a  $D$  candidate as having valid vertex reconstruction if it is formed by at least two tracks with hits in the silicon vertex detector. To suppress feed-down from the Cabibbo allowed decay  $\bar{B}^0 \rightarrow D^{*+} D_s^{(*)-}$  due to  $K/\pi$  misidentification, we apply a  $D_s^-$  veto for the  $D^- \rightarrow K^+\pi^-\pi^-$  and  $K_S\pi^-$  channels: if a pion candidate can also be identified as a kaon, and if, after reassignment of the kaon mass, the invariant mass of the combination is within  $\pm 15 \text{ MeV}/c^2$  of the nominal  $D_s^-$  mass, the combination is rejected. This requirement suppresses the  $\bar{B}^0 \rightarrow D^{*+} D_s^{(*)-}$  background by a factor of 10 with signal efficiency of 98%. The  $D^{*+}$  candidates are formed from  $D^0 \pi_{\text{slow}}^+$  combinations with invariant masses within  $\pm 2 \text{ MeV}/c^2$  of the nominal  $D^{*+}$  mass.

In the full reconstruction method we define  $B^0$  candidates as combinations of oppositely charged  $D^{*+}$  and  $D^-$  candidates, where at least one of the  $D^-$  or the  $D^0$  from the  $D^{*+}$  decay has valid vertex reconstruction. The signal is identified using the c.m. system energy difference  $\Delta E = E_B^* - E_{\text{beam}}$  and the beam-energy constrained mass  $M_{\text{bc}} = \sqrt{E_{\text{beam}}^2 - P_B^{*2}}$ , where  $E_B^*$  ( $P_B^*$ ) is the energy (momentum) of the  $B$  candidate in the c.m. and  $E_{\text{beam}}$  is the c.m. beam energy.  $B^0$  candidates are preselected by requiring  $|\Delta E| < 100 \text{ MeV}$  and  $M_{\text{bc}} > 5.21 \text{ GeV}/c^2$ . In case of multiple  $B^0$  candidates in this region a single candidate per event is selected based on the minimum sum of  $\chi^2/\text{DOF}$  of the fits to intermediate charmed mesons. The scatter plot of  $\Delta E$  vs.  $M_{\text{bc}}$  and the  $\Delta E$  and  $M_{\text{bc}}$  projections are shown in Figs. 1. In the  $M_{\text{bc}}$  projection  $B^0$  candidates are selected from the  $|\Delta E| < 20 \text{ MeV}$  region; the  $\Delta E$  distribution is plotted for the region  $M_{\text{bc}} > 5.27 \text{ GeV}/c^2$ . A fit to the  $M_{\text{bc}}$  distribution with a Gaussian representing the signal contribution and an ARGUS function [9]

parameterizing the background finds a signal yield of  $161 \pm 16$  events. A fit to the  $\Delta E$  distribution is performed using a double Gaussian to parameterize the signal, while the background is described by a linear function. This fit yields  $149 \pm 18$  signal events. The  $\cos \theta$  distribution, where  $\theta$  is a decay angle in the  $D^{*+}$  rest frame relative to the boost direction, for the candidates from the  $|\Delta E| < 20 \text{ MeV}$  and  $M_{bc} > 5.27 \text{ GeV}/c^2$  region determined from  $M_{bc}$  fits is shown in Fig. 1 d) and is in good agreement with the Monte Carlo (MC) expectation.

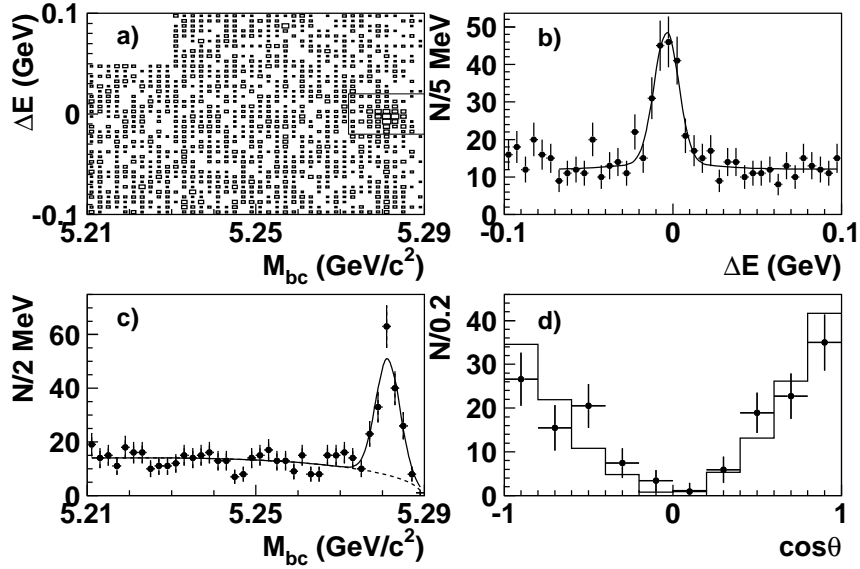


FIG. 1: Kinematic distributions of  $B^0 \rightarrow D^{*+} D^-$  candidates: a) scatter plot of  $\Delta E$  vs.  $M_{bc}$ , b), c)  $\Delta E$  and  $M_{bc}$  projections, d)  $\cos \theta$  determined from  $M_{bc}$  fits in the data (points with error bars) and in the signal MC (histogram). The curves represent the fit described in the text.

In the partial reconstruction analysis we define  $B$  candidates as combinations of  $D^-$  with valid vertex reconstruction and  $\pi_{\text{slow}}^+$ . As in our previous publication [3], the angle  $\alpha$  between the  $D^-$  and  $\pi_{\text{slow}}^+$  c.m. momenta, and the  $D^{*+}$  helicity angle  $\theta$ , calculated using kinematic constraints, are used to identify the studied decay. We use the  $D^- \rightarrow K^+ \pi^- \pi^-$  decay mode only. In addition, the  $D^-$  c.m. momentum is required to lie in the interval  $1.63 \text{ GeV}/c < P_{D^-}^* < 1.97 \text{ GeV}/c$ , and the c.m. momentum of  $\pi_{\text{slow}}^+$  is required to be smaller than  $0.2 \text{ GeV}/c$ . Both momentum intervals correspond to the kinematic limits for the studied decay. In order to make the fully and partially reconstructed samples statistically independent,  $\pi_{\text{slow}}^+$  is rejected if, after being combined with any  $D^0$  in the event, it forms a  $D^{*+}$  candidate. The presence of a lepton ( $\ell_{\text{tag}}$ ) in the event is required to pro-

vide flavor tagging, suppress the continuum background to a negligible level, and also reduce the combinatorial  $B\bar{B}$  background. Charged tracks with c.m. momenta in the range  $1.1 \text{ GeV}/c < P_{\ell_{\text{tag}}}^* < 2.3 \text{ GeV}/c$ , which are identified as muons or electrons are considered as leptons. A large fraction of the selected  $D^-\ell_{\text{tag}}$  combinations originate from the decay of the same  $B$  meson:  $B \rightarrow D^-\ell^+X$ . This background is removed by a kinematic requirement that  $D^-$  and  $\ell_{\text{tag}}$  do not originate from the same  $B$ :

$$\frac{(E_{\text{beam}} - E_{D\ell_{\text{tag}}}^*)^2 - P_B^{*2} - P_{D\ell_{\text{tag}}}^{*2}}{2P_B^*P_{D\ell_{\text{tag}}}^*} < -1.1, \quad (3)$$

where  $E_{D\ell_{\text{tag}}}^*$  ( $P_{D\ell_{\text{tag}}}^*$ ) is the c.m. energy (momentum) of the  $D^-\ell_{\text{tag}}$  combination. The efficiency of this requirement for the signal is estimated from MC simulation to be 87%, while the background is suppressed by a factor greater than 2. This requirement also removes leptons produced from the unreconstructed  $D^0$  in the signal decay, an additional source of mistagging. We select partially reconstructed  $B^0$  candidates by requiring  $\cos\alpha < 0$  and  $|\cos\theta| < 1.05$ . In case of multiple candidates, the  $D^-\pi_{\text{slow}}^+$  combination with the best probability of the  $D^-$  vertex fit or the largest  $|\cos\theta|$  is selected. The expected number of signal events in the partial reconstruction sample is calculated from the full reconstruction signal yield relying on the MC ratio of full and partial reconstruction efficiencies. We estimate  $N_{\text{partial}} = 133 \pm 13$  and use this number to fix the signal fraction in later fits.

We cross-check this result by estimating the signal fraction from the data. The distributions of  $\cos\alpha$  for two regions of  $\cos\theta$  are shown in Fig. 2, after imposing a tight requirement of  $\pm 8 \text{ MeV}/c^2$  ( $\sim 2\sigma$ ) on the  $D^-$  mass. The first region  $0.50 < |\cos\theta| < 1.05$  (Fig. 2 a)) is signal enriched due to the  $D^{*+}$  polarization; the second region  $|\cos\theta| < 0.50$  (Fig. 2 b)) is dominated by background. In a simultaneous fit to the two  $\cos\alpha$  distributions the signal shapes are fixed from the MC. The combinatorial background is parameterized by a second order polynomial function. The contributions from  $\bar{B}^0 \rightarrow D^{*+}D_s^{(*)-}$  and  $B^0 \rightarrow D^{*+}D^{*-}$  are fixed from the MC simulation. The fit yields  $137 \pm 39$  signal events, in good agreement with the yield expected from the full reconstruction analysis.

In the full reconstruction method, charged tracks that are not associated with the reconstructed  $B^0 \rightarrow D^{\pm}D^{\mp}$  are used to identify the flavor of the signal  $B^0$  [10]. Events are divided into six subsamples of the parameter  $r$ , which is an event-by-event, MC-determined flavor-tagging quality factor that ranges from  $r = 0$  for no flavor discrimination to  $r = 1$  for unambiguous flavor assignment. The wrong-tag fraction and difference between  $B^0$  and  $\bar{B}^0$

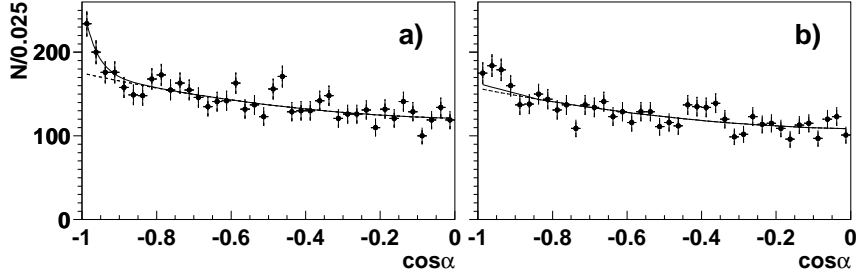


FIG. 2: Distributions of  $\cos \alpha$  for: a)  $0.50 < |\cos \theta| < 1.05$ ; b)  $|\cos \theta| < 0.50$ . The fit functions are shown with solid lines; the combinatorial backgrounds are presented by dashed lines.

decays in each interval ( $w_i$  and  $\Delta w_i$ ,  $i = 1, 6$ ) are fixed using a data sample of self-tagged  $B^0$  decay modes. In the partial reconstruction case, flavor tagging is provided by the high momentum lepton required in the event; the wrong tag fraction is determined from data as discussed below.

The proper-time difference between the reconstructed and tagged  $B$  decay is calculated as  $\Delta t = (z_{D^*D} - z_{\text{tag}})/\beta\gamma c$ , where  $z_{D^*D}$  and  $z_{\text{tag}}$  are the  $z$  coordinates of the two  $B$  decay vertices and  $\beta\gamma = 0.425$  is the Lorentz boost factor at KEKB. In the full reconstruction method we determine the  $B^0$  signal vertex by fitting the momentum vectors of  $D^-$  and/or  $D^0$  candidates with well-reconstructed vertices with the constraint of the interaction region profile. The tagging  $B$  vertex is found using well reconstructed charged tracks not assigned to the signal  $B^0$  and excluding tracks that form a  $K_S$  candidate. The signal resolution function parameters are obtained from the  $\Delta t$  fit to the  $B^0$  lifetime for the events from the signal region. The tagging  $B^0$  vertex resolution function is fixed from [10]. In the partial reconstruction method, the signal and tagging  $B^0$  vertices are reconstructed using the  $D^-$  candidate and  $\ell_{\text{tag}}$ , respectively. In this case, both the resolution function parameters and the wrong tag fraction are extracted from the data using a sample of  $B^0 \rightarrow D^- \ell^+ \nu X$  decays tagged with a high momentum lepton. The  $D^- \ell^+$  combinations are required to originate from the same  $B$  decay based on the recoil mass against the  $D^- \ell^+$  system and its c.m. momentum. The selected  $D^- \ell^+$  combinations are almost pure  $B^0 \rightarrow D^- \ell^+ \nu$  signal events with a small admixture of  $B^0 \rightarrow D^{*-}(D^- \pi^0) \ell^+ \nu$ ; the latter process is also considered as signal. A small contribution from combinatorial background under the  $D^-$  peak is estimated using  $D^-$  mass sidebands. The  $D^-$ ,  $\ell^+$  and  $\ell_{\text{tag}}$  vertices ( $z_{D^-}$ ,  $z_{\ell^+}$  and  $z_{\ell_{\text{tag}}}$ ) are reconstructed using identical procedures to those used in the partial reconstruction method. The resolution

function is extracted from an unbinned maximum likelihood fit to the  $\Delta t_\ell \equiv (z_{D^-} - z_\ell)/\beta\gamma c$  distribution. The wrong tag fraction is found from a fit to  $\Delta t_{\text{tag}} \equiv (z_{D^-} - z_{\text{tag}})/\beta\gamma c$  to be  $w = 6.1 \pm 0.9\%$ . As a cross-check, the  $B^0$  lifetime and mixing parameter  $\Delta m_d$  are also measured from the fit to the  $\Delta t_{\text{tag}}$  distribution to be  $1.48 \pm 0.04 \text{ ps}$  and  $0.52 \pm 0.02 \text{ ps}^{-1}$ , respectively, consistent with [11].

In the full reconstruction method, the signal region is defined as  $|\Delta E| < 50 \text{ MeV}$  and  $M_{\text{bc}} > 5.27 \text{ GeV}/c^2$ , and contains 360 events with 46% signal purity. In the partial reconstruction method, the signal region is chosen as  $|M_{K^+\pi^-\pi^-} - M_{D^-}| < 15 \text{ MeV}/c^2$ ,  $\cos \alpha < -0.9$  and  $|\cos \theta| < 1.05$ . The total number of selected events is 2174 with 6% signal purity.

We determine the  $CP$  violation parameters from an unbinned maximum likelihood fit to the  $\Delta t$  distribution. The signal probability density function is given by Eq. 1 with effects due to mistagging taken into account. The resolution function  $R_{D^*D}$  is formed by convolving four components: the detector resolutions for  $z_{D^*D}$  and  $z_{\text{tag}}$ , the shift in the  $z_{\text{tag}}$  vertex position due to secondary tracks originating from charmed particle decays, and the smearing due to the kinematic approximation used to convert  $\Delta z$  to  $\Delta t$  [10]. For each event we define the following likelihood value

$$P_i = \int \left[ \frac{f_{D^*D}}{f_{D^*D} + f_{\text{bg}}} \mathcal{P}_{D^*D}(\Delta t') R_{D^*D}(\Delta t_i - \Delta t') + \frac{f_{\text{bg}}}{f_{D^*D} + f_{\text{bg}}} \mathcal{P}_{\text{bg}}(\Delta t') R_{\text{bg}}(\Delta t_i - \Delta t') \right] d\Delta t', \quad (4)$$

where signal ( $f_{D^*D}$ ) and background ( $f_{\text{bg}}$ ) fractions are calculated as functions of the following variables:  $\Delta E$  and  $M_{\text{bc}}$  (full reconstruction);  $M_{D^-}$  and  $\cos \alpha$  (partial reconstruction);  $\cos \theta$  (both cases). The signal distributions of the variables used for  $f_{D^*D}$  parametrization are determined from the MC simulation. The background parameters are obtained from the data.

In the full reconstruction, the background  $\Delta t$  shape is fixed using the large  $M_{\text{bc}}\text{-}\Delta E$  region excluding the signal region. For the partial reconstruction the background contains a combinatorial component, for which the shape is obtained from  $D^-$  mass sidebands ( $30 \text{ MeV}/c^2 < |M_{K^+\pi^-\pi^-} - M_{D^-}| < 60 \text{ MeV}/c^2$ ), and a component containing a real  $D^-$ , which may come from  $B$  decay. The shape of the latter includes a mixing term, and is obtained from a sideband ( $-0.8 < \cos \alpha < 0.0$ ).

Finally, the results for the  $CP$  violation parameters  $\mathcal{A}$ ,  $S_\pm$ , and  $C_\pm$  obtained from the

TABLE I: Fit results.

	full rec.	partial rec.	combined
$\mathcal{A}$	$+0.03 \pm 0.09$	$+0.16 \pm 0.18$	$+0.07 \pm 0.08$
$S_-$	$-1.17 \pm 0.48$	$-0.65 \pm 0.79$	$-0.96 \pm 0.43$
$C_-$	$+0.33 \pm 0.29$	$+0.11 \pm 0.45$	$+0.23 \pm 0.25$
$S_+$	$-0.25 \pm 0.52$	$-0.92 \pm 0.58$	$-0.55 \pm 0.39$
$C_+$	$-0.34 \pm 0.27$	$-0.39 \pm 0.38$	$-0.37 \pm 0.22$

individual fits to the statistically independent full reconstruction and partial reconstruction samples, as well as the result of the combined fit, are summarized in Table I. We calculate the combined statistical significance of  $CP$  violation to be  $2.7\sigma$ . The significance is defined as  $\sqrt{-2\ln(L_0/L_{\max})}$ , where  $L_{\max}$  is the likelihood returned by the combined fit and  $L_0$  is determined from a fit with the parameters  $\mathcal{A}$ ,  $S_{\pm}$  and  $C_{\pm}$  constrained to the values corresponding to no  $CP$  violation:  $\mathcal{A} = 0$ ,  $S_+ = -S_-$  and  $C_+ = -C_-$ .

The  $\Delta t$  distributions for the subsamples having the best signal and tagging quality ( $f_{D^*D} > 0.1$  and  $r > 0.5$ ) after background subtraction are shown in Fig. 3 a) and b) for the full and partial reconstruction methods, respectively.

The systematic error is dominated by the uncertainties in the signal fraction ( $\pm 0.07$  for  $S_{\pm}$  and  $\pm 0.03$  for  $C_{\pm}$ ), wrong tag fraction ( $\pm 0.05$  for  $S_{\pm}$  and  $\pm 0.03$  for  $C_{\pm}$ ), resolution function parameterization ( $\pm 0.05$  for  $S_{\pm}$  and  $\pm 0.02$  for  $C_{\pm}$ ) and vertexing ( $\pm 0.05$  for  $S_{\pm}$  and  $\pm 0.01$  for  $C_{\pm}$ ). Other contributions come from the correlated backgrounds and signal box definition. The result is consistent with [4]. We perform a number of cross-checks for our measurement. Using an ensemble of MC pseudo-experiments, we check both the linearity of the fitting procedure and the reliability of the statistical errors returned by the  $CP$  fit. A similar  $CP$  violation study is performed with self-tagged  $\bar{B}^0 \rightarrow D^{*+} D_s^-$  decay using both full and partial reconstruction techniques. The combined fit yields  $\mathcal{A} = 0.00 \pm 0.03$ ,  $S_- = +0.08 \pm 0.12$ ,  $C_- = -1.11 \pm 0.07$ ,  $S_+ = +0.00 \pm 0.12$ , and  $C_+ = +1.12 \pm 0.07$ , consistent with the expected values  $\mathcal{A} = 0$ ,  $S_{\pm} = 0$  and  $C_+ = -C_- = 1$ .

In summary, we have performed a search for the  $CP$ -violating asymmetry in the decay

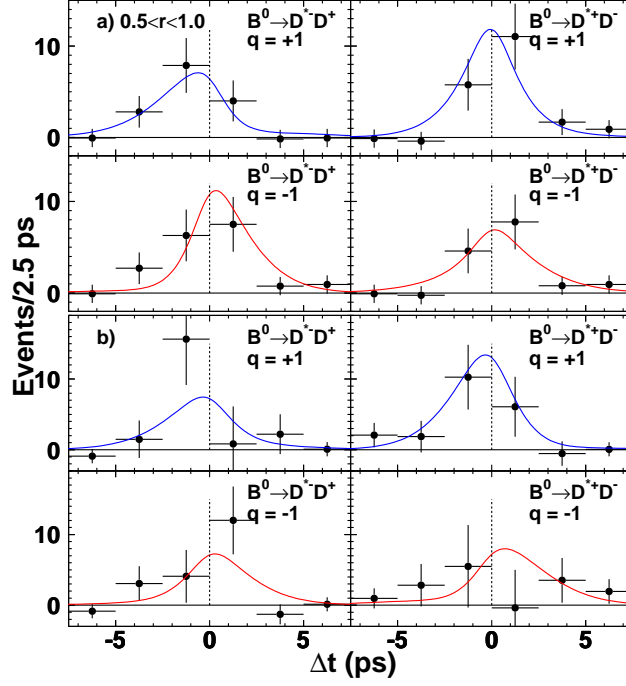


FIG. 3: Background subtracted  $\Delta t$  distributions in the a) full and b) partial reconstruction methods. The curves show the result of the fits.

$B^0 \rightarrow D^{*\pm} D^\mp$  using two methods of  $B^0$  reconstruction. From the combined fit to the data we have measured  $\mathcal{A} = +0.07 \pm 0.08 \pm 0.04$ ,  $S_- = -0.96 \pm 0.43 \pm 0.12$ ,  $C_- = +0.23 \pm 0.25 \pm 0.06$ ,  $S_+ = -0.55 \pm 0.39 \pm 0.12$  and  $C_+ = -0.37 \pm 0.22 \pm 0.06$ . These are the most precise measurements of these parameters to date. The significance of nonzero  $CP$  violation in  $B^0 \rightarrow D^{*\pm} D^\mp$  is  $2.7\sigma$ .

We thank the KEKB group for the excellent operation of the accelerator, the KEK Cryogenics group for the efficient operation of the solenoid, and the KEK computer group and the NII for valuable computing and Super-SINET network support. We acknowledge support from MEXT and JSPS (Japan); ARC and DEST (Australia); NSFC (contract No. 10175071, China); DST (India); the BK21 program of MOEHRD and the CHEP SRC program of KOSEF (Korea); KBN (contract No. 2P03B 01324, Poland); MIST (Russia); MESS (Slovenia); NSC and MOE (Taiwan); and DOE (USA).

---

[1] M. Kobayashi and T. Maskawa, Prog. Theor. Phys. **49** 652 (1973).

- [2] R. Aleksan *et al.*, Phys. Lett. B **317**, 173 (1993).
- [3] Belle Collaboration, K. Abe *et al.*, Phys. Rev. Lett. **89**, 122001 (2002).
- [4] *BABAR* Collaboration, B. Aubert *et al.*, Phys. Rev. Lett. **90**, 221801 (2003).
- [5] Z.-Z. Xing, Phys. Lett. B **443**, 365 (1998).
- [6] Belle Collaboration, A. Abashian *et al.*, Nucl. Instrum. Methods Phys. Res., Sect. A **479**, 117 (2002).
- [7] S. Kurokawa and E. Kikutani, Nucl. Instrum. Methods Phys. Res., Sect. A **499**, 1 (2003).
- [8] The inclusion of charge conjugate modes is implied through this Letter.
- [9] ARGUS collaboration, H. Albrecht *et al.*, Phys. Lett. B **229**, 304 (1989).
- [10] Belle Collaboration, K. Abe *et al.*, hep-ex/0308036; Belle Collaboration, H. Kakuno *et al.*, hep-ex/0403022; Belle Collaboration, K. Abe *et al.*, Phys. Rev. D **66**, 071102 (2002).
- [11] S. Eidelman *et al.*, Phys. Lett. B **592**, 1 (2004).